Validity of the perturbation theory for hard particle systems with very-short-range attraction

Ph. Germain* and S. Amokrane
Groupe de Physique des Milieux Denses, Faculté des Sciences et de Technologie, Université Paris XII, 61 Avenue du Général de Gaulle, 94010 Créteil Cedex, France
(Received 20 July 2001; published 6 March 2002)

Motivated by recent studies of colloidal systems at the effective one-component level, the validity of the first-order perturbation theory of classical systems of hard particles interacting via short-range potentials is investigated. The influence of the physical parameters on the accuracy of the perturbation theory is examined. It is shown that this simple method is intrinsically appropriate to describe the fluid-solid transition. Concerning the fluid-fluid one, the first-order perturbation theory provides acceptable results when the interaction range is not too small. For very-short-range potentials it systematically leads to an unphysical fluid-fluid transition. In the case of the depletion interaction between hard sphere solutes such a transition is found even at moderate size asymmetry. It is finally shown that the perturbation theory is not more appropriate for an extended solid than for a liquid with the same density, thus making difficult a quantitative description of the isostructural solid-solid transition.

DOI: 10.1103/PhysRevE.65.031109 PACS number(s): 05.20.−y, 64.60.−i, 82.70.−y

I. INTRODUCTION

In recent years, the theoretical study of systems of classical particles interacting via short-ranged potentials has become a relevant issue with a view to understanding the behavior of supramolecular systems, such as fullerenes or colloids. For fullerenes, the unusually narrow attractive part of the interaction [1] with respect to simple (Lennard-Jones-like) fluids leads to an extreme reduction of the stability domain of the liquid phase, or even to its complete suppression according to some theoretical studies (see [2,3] and references therein). In the case of colloids, the occurrence of a short-range effective attraction between solute particles (the so called depletion potential) was already predicted by Asakura and Oosawa [4] by modeling the suspension as an asymmetric binary mixture of pure hard spheres (HS). The depth and range of the depletion well is determined by the solvent density and the diameter of the small spheres: the range is therefore extremely small for colloids dispersed in a true solvent, and more variable for mixtures of two distinct supramolecular solutes. For HS mixtures with sufficiently high size ratio and solvent density, this attraction is responsible for the phase separation that Biben and Hansen [5] predicted from the Ornstein-Zernike equations (OZE's) with particular closures for the pair distribution functions (PDF). This possibility, in contradiction with the long shared conclusion of Lebowitz and Rowlinson [6], has given a new impetus to the study of these mixtures in two equally relevant directions: (i) the accurate determination of the depletion potential (first for the HS mixture, and next for more realistic models), (ii) the search of suitable theoretical methods for treating such interactions. The latter point is our main concern in this work.

Point (i) has been considered several times in the literature: the potential of mean force between large solute spheres has been investigated by various methods including density expansion [7–9], calculation of the effective force in the superposition approximation [10–12], approximate closures of the OZE [13–15], and also numerical simulation [11,16–18]. While confirming some aspects of the simple calculation of Asakura and Oosawa, these calculations lead to a more complex picture of the depletion potential: it has a deeper and narrower attractive well, followed by oscillations with a period roughly equal to the small sphere's diameter, and related to the incorporation of a hard core repulsion between the small spheres. On the other hand, recent works have underlined the necessity to go beyond hard spheres in order to describe real systems, especially pure colloid-solvent mixtures (see [12,15,19–21] and references on experimental works therein).

Therefore, the question of the appropriate model of the potential of mean force for colloids is still open. But, it already appears that the interaction should be in any case ''singular,'' that is, extremely short ranged and oscillatory, with respect to simple fluids. Therefore, it is necessary to determine which theoretical methods are suitable in this case.

For the fluid state, integral equations of the reference hypernetted chain (RHNC) type [22] appear to be powerful enough, at least at the level of the effective one-component fluid, to reproduce the results of numerical simulations [15] (see also [23,24] for simple fluids). However, this method requires heavy computations, and is severely limited by the presence of a region of the phase diagram, close to the fluid-fluid (F-F) transition line, where numerical convergence is impossible. Moreover, it does not permit a simple understanding of the influence of the various parameters of the model. In contrast, the much simpler perturbation theory presents just the opposite characteristics: it involves faster calculations, lends itself to simpler interpretations, but has a more uncertain domain of validity.

For the solid, the situation is even more complex because the loss of translation invariance prohibits in practise the use of integral equations. Various density functional methods have then been proposed. Among these, the modified

*Author to whom correspondence should be addressed. Email address: germain@univ-paris12.fr

weighted density approximation (MWDA) of Denton and Ashcroft [25] provides a consistent–and nonperturbative–calculation of the phase diagram, by extracting the free energy of the solid by reference to the fluid state. Unfortunately, this method and its variants suffer from difficulties in the treatment of attractive tails, and for all solids at high density [26–29]. It is, therefore, not appropriate for colloids since the very short range of the depletion potential may induce a melting or solid-solid (S-S) transition near close packing (see Sec. IV).

Therefore, as a fully consistent treatment by using the fluid state as unique reference is not feasible for the present systems, an alternative could be to use approximations specific to the high-density limit. In this way, an improved MWDA was proposed recently for repulsive potentials, incorporating also the properties of the static solid and a model of the lattice vibrations [29]. Alternatively, in Ref. [15], the HS binary mixture was studied in the one-component representation by employing a hybrid method: the RHNC closure was used for the fluid phase, while the solid one was studied by a simple first-order perturbation theory (FPT) with the HS potential as reference. For the typical size ratio $q=10$, this apparently rough treatment of the solid led to a remarkable agreement with the MC results [17] for the fluid-solid (F-S) transition, both in the low solvent density regime and the high-density one. In contrast, the extension of the FPT to the fluid phase [30] gave much more contrasted results: while the F-S transition lines remain quite correctly reproduced, an unphysical F-F transition is systematically found at very high density, in complete contradiction with numerical simulations. Concerning the S-S transition, which is stable for $q \geqslant 20$ [17], the high-density branch (near close packing) obtained in the FPT is very close to the MC points. But the agreement clearly worsens for the lower-density one. Previously, the FPT has been applied to the attractive Yukawa HS systems [31,32] and compared to simulations [31,33] for different attraction range parameters κ. The trends observed were similar to those relative to the depletion potential: better agreement with the MC results for the F-S transition than for the F-F and S-S ones (the latter existing for $\kappa > 25$ [33]). However, for the F-F transition, the discrepancies were much less dramatic than for the depletion potential and only quantitative: the F-F coexistence domain was simply overestimated for $\kappa = 2-9$, the F-F line being stable in the FTP for κ smaller than about 7.4 instead of 6 in the MC simulations [32].

To summarize, the scope of this paper is to investigate the conditions of validity of the FPT in the fluid and solid states, and to evaluate the consequences of this simple approximation according to the physical system under consideration. In Sec. II, we recall briefly the HS perturbation scheme, and we discuss at qualitative level the influence of the physical parameters on the accuracy of the FPT. In Sec. III, we present the method used to test this approximation numerically. In Sec. IV, we present our results for two typical interaction potentials: the Yukawa one and a model of the depletion one. We provide a consistent explanation of the results obtained so far in the literature. In particular, we point out the consequence of the FPT on the F-F and S-S transitions when the attraction has an extremely short range. Sec. V is the conclusion.

II. PERTURBATION TREATMENT OF THE FREE ENERGY

A. General expression of the excess free energy

The principle of the perturbation calculation with respect to the interacting potential is to derive an approximate expression of the total free energy F from the exact relation [34],

$$\beta F = \beta F_0 + \int_0^\beta U(\beta) d\beta, \tag{1}$$

where F_0 is the free energy of the hard sphere reference system (whose properties are assumed to be known), $\beta = 1/k_B T$ with T the temperature, and $U(\beta)$ the internal energy of the system calculated for the total potential. By defining $F_1 = F - F_0$ as the excess free energy due to the perturbation potential, Eq. (1) leads to

$$\beta F_1 = \beta U_0 + \sum_{n \geqslant 1} \frac{\beta^{n+1}}{(n+1)!} \left(\frac{\partial^n U}{\partial \beta^n} \right)_{\beta=0}, \tag{2}$$

with $U_0 = U(\beta = 0)$. As the values of U and its derivatives are computed at infinite temperature, they involve only the distribution functions of the HS reference system, and do not depend on β. Equation (2) is thus the high-temperature expansion of the free energy, whose lowest-order terms read

$$\beta F_1 = \beta \langle W_N \rangle_0 (1 - \Delta_2) + O((\beta W_N)^3), \tag{3}$$

$$\Delta_2 = \frac{\beta(\langle W_N^2 \rangle_0 - \langle W_N \rangle_0^2)}{\langle W_N \rangle_0},$$

W_N being the N body perturbation potential (after subtraction of the core repulsion), and the symbol $\langle\ \rangle_0$ denoting the statistical averages calculated in the reference HS system. $\langle W_N \rangle_0$ is thus the total perturbation energy, while the higher-order terms are determined by its fluctuations. For a pairwise additive potential [$W_N = \Sigma_{i<j} V(r_{ij})$ with $V(r)$ the pair interaction outside the core], $\langle W_N \rangle_0$ reduces to

$$\langle W_N \rangle_0 = \frac{1}{2} \int \int d\mathbf{r}\, d\mathbf{r}'\, \rho_0^{(2)}(\mathbf{r}, \mathbf{r}') V(|\mathbf{r} - \mathbf{r}'|), \tag{4}$$

with $\rho_0^{(2)}(\mathbf{r}, \mathbf{r}')$ the HS two-particle density. In contrast, the next term, containing contributions from $V(|\mathbf{r} - \mathbf{r}'|) \times V(|\mathbf{r}'' - \mathbf{r}'''|)$, is much more complex since it also involves the three- and four-particle densities of the reference system, etc. (the calculation of the term in β^n requires the knowledge of all the distribution functions up to order $2n$).

Therefore, although the temperature expansion (2) can be performed in principle to any order, it is rather used in practice when the terms beyond first order are negligible. In this case one simply writes $F_1^{\text{pert}} = F_0 + \langle W_N \rangle_0$, where $\langle W_N \rangle_0$ is

given by Eq. (4). The validity of such an approximation may be discussed by considering the ratio Δ_2 or, equivalently, by reexpressing Eq. (1) as

$$F = F_0 + \frac{1}{2}\int_0^1 d\lambda \int\int d\mathbf{r}\, d\mathbf{r}'\, \rho_\lambda^{(2)}(\mathbf{r},\mathbf{r}')V(|\mathbf{r}-\mathbf{r}'|), \quad (5)$$

with $\rho_\lambda^{(2)}(\mathbf{r},\mathbf{r}')$ the two-particle density for $V_\lambda = \lambda V$. Equations (4) and (5) show that the FPT amounts to replacing $\rho_\lambda^{(2)}(\mathbf{r},\mathbf{r}')$ by $\rho_0^{(2)}(\mathbf{r},\mathbf{r}')$ in the charging process, and thus to neglect the variations of the pair correlation function induced by the perturbation potential. The part of the free energy neglected in this approximation is therefore

$$\beta\Delta F_1 = \frac{1}{2}\int_0^1 d\lambda \int\int d\mathbf{r}\, d\mathbf{r}'[\rho_\lambda^{(2)}(\mathbf{r},\mathbf{r}') - \rho_0^{(2)}(\mathbf{r},\mathbf{r}')]V(|\mathbf{r}-\mathbf{r}'|). \quad (6)$$

B. Accuracy of the first-order perturbation theory

As emphasized in the Introduction, the application of the FPT to very-short-ranged interaction, such as in colloids or Yukawa systems with large screening parameters, has given contrasting results according to the specific transition under consideration [30–33]. To gain some understanding of this situation, it is useful to try to specify the physical parameters that determine its validity. This discussion will facilitate the interpretation of the quantitative results presented in Sec. IV.

The perturbation potentials considered in the literature are often of the form $\beta V(r) = \varepsilon^* f(r/\sigma)$ with σ a suitably defined HS diameter. The magnitude of $\beta\Delta F_1$ is then essentially determined by three parameters (see also [34]).

(1) The reduced interaction strength ε^*. One has indeed $\Delta_2 \sim \varepsilon^*$ (and thus $\beta\Delta F_1 \sim \varepsilon^{*2}$). Δ_2 is therefore small with respect to 1 when ε^* is small enough. This is the typical case for which the FPT is appropriate [see Eqs. (2) and (3)]. This explains why it usually reproduces correctly the *F-S* (HS-like) transition in the supercritical region.

(2) The density ρ of the system. $\beta\Delta F_1$ vanishes in the two opposite limits $(\rho \to 0)$ and $(\rho \to \rho_c)$ with ρ_c the close packing density ($\rho_c = \sqrt{2}/\sigma^3$ with σ the HS diameter). For $\rho \to 0$, this is a simple consequence of the behavior in ρ^2 of the excess free energy, leading in every case to a small contribution. In the opposite limit $(\rho \to \rho_c)$, $\beta\Delta F_1$ also vanishes because correlations are dominated by the core effects, as a consequence of the reduction of the free volume. In this limit, the HS distribution function shows a high and narrow peak near contact. When the width of this peak is small enough with respect to the distance over which $V(r)$ varies, the effect induced by the charging process on $\rho_\lambda^{(2)}(\mathbf{r},\mathbf{r}')$ is expected to be weak, the equality $\rho_\lambda^{(2)}(\mathbf{r},\mathbf{r}') = \rho_0^{(2)}(\mathbf{r},\mathbf{r}')$ being exactly satisfied at close packing [35]. We wish to emphasize that, in this part of the phase diagram, the relevant parameter for the accuracy of the FPT is the density of the system, and not its thermodynamic state (liquid or solid). It is indeed commonly argued that the FTP should be appropriate especially for a solid with the lattice spacing larger than that of the range of the interaction (see for instance [30,34,36]). In fact, this argument considers only a static solid, for which one has $\rho^{(2)}(\mathbf{r},\mathbf{r}') = \rho(\mathbf{r})\rho(\mathbf{r}')$. In a real solid, not at close packing, the averaged PDF $\overline{g_0}(r)$ of the HS reference system shows a peak near contact whose width decreases with density (see, for example, Fig. 1 in Ref. [37] or [38]) as in the liquid state. Therefore, the validity of the FPT does not depend intrinsically on the nature of the thermodynamic state, but rather on the density. As we will see in the Sec. IV, $\beta\Delta F_1$ is not necessarily smaller, for a given density, for the solid state than for the liquid one.

It appears from (1) and (2) that, whatever $V(r)$ is, the regions of the phase diagram where the FPT is more appropriate are the supercritical region and the two opposite domains $(\rho \to 0)$ and $(\rho \to \rho_c)$. This corresponds to the *F-S* transition, which involves states belonging all to one of these regions: high temperature for the HS-like part of the transition, and extreme densities for the low-temperature gas-dense solid transition. On the contrary, the *F-F* and the *S-S* transitions (when the latter exists) require a sizeable value of the reduced strength ε^* and involve states with intermediate density: the liquid state for the *F-F* transition, and the low-density solid state for the *S-S* one. With some interaction potentials, the FPT has failed precisely for these transitions. For intermediate densities, indeed, the validity of the FPT depends strongly on the range of $V(r)$.

(3) The range of the potential. The numerical evaluation of $\beta\Delta F_1$ (see Sec. IV) shows that the range of the function $f(r/\sigma)$ has opposite effects at low or high density. At low density, using the reasonable approximation $g_\lambda(r) \simeq \Theta(r/\sigma - 1)\exp[-\lambda\varepsilon^* f(r/\sigma)]$ [with $\Theta(x)$ the Heavyside step function], one gets

$$\frac{\beta\Delta F_1}{N} \simeq 12\eta \int_1^\infty dx \left(\frac{1-\exp[\varepsilon^* f(x)]}{\varepsilon^* f(x)} - 1 \right),$$

in which the integrand vanishes outside the attractive region of $f(x)$. Therefore, the deviation $\beta\Delta F_1$ is the smaller the shorter is the range of $f(x)$. At high density, one has the opposite trend: indeed, as pointed out in (2) the condition $\rho_\lambda^{(2)}(\mathbf{r},\mathbf{r}') \simeq \rho_0^{(2)}(\mathbf{r},\mathbf{r}')$ is satisfied only when the variation of $f(x)$ (in the region of contact) is slow enough with respect to that of $g_0(x)$ [or $\overline{g_0}(x)$ for the solid state]. Therefore, starting from ρ_c, the domain of density for which the perturbation treatment is valid reduces when the range of the interaction is decreased. This point is important for understanding why the failures of the FTP are especially important in the case of asymmetric HS mixtures.

To close this section, we note that our discussion of the high-density limit is restricted to the case of interaction potential having a hard-core part. For potentials with soft-core repulsion, the FPT with HS reference system is inaccurate at high density (see discussion in Ref. [39] and references therein). Indeed, the starting Eqs. (1)–(3) are valid only when both the total and the reference potential have the same ensemble of accessible states in the phase space. When this is not so, entropy effects are incorrectly accounted for at high density.

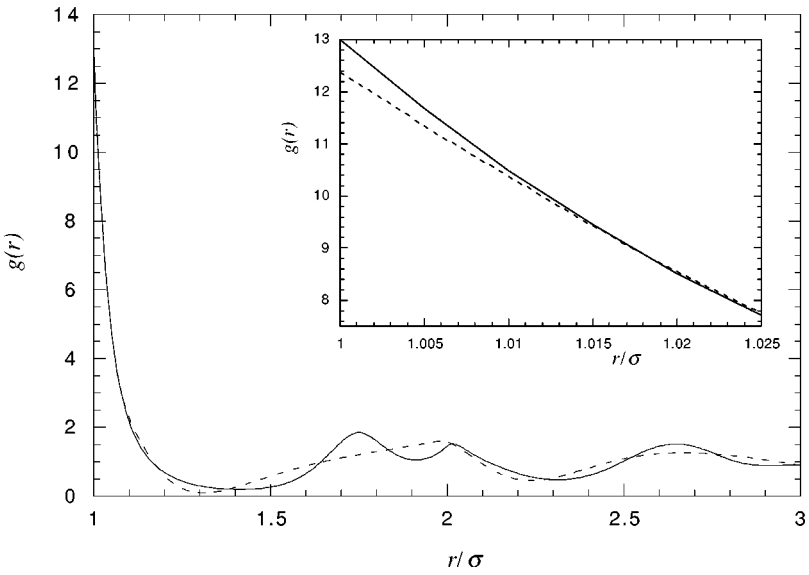

FIG. 1. Pair distribution functions of the hard sphere fluid ($\eta=0.62$) computed from the Verlet-Weis parametrization (dashed line) and from the Malijevski-Labik parametrization (solid line). Inset shows the region of contact.

III. OUTLINE OF THE METHOD

Before presenting our comparison of the FPT with exact results in the fluid and in the solid (see next section), we first detail the method used for each state. This will be applied for the Yukawa and for the Goëtzman-Evans-Dietrich (GED) potential [8].

In the fluid, $\beta\Delta F_1$ was computed by using as the "exact" free energy F given by the RHNC theory, with optimized reference system [22]. This method is indeed known to very accurately reproduce simulation data for many simple fluids such as the LJ [23] or Yukawa [24] fluids. Recently, good agreement with simulations was also found for binary HS mixtures, in the effective one-component fluid representation, at several values of solvent densities and size ratios [15]. This method being well known, we briefly recall here the main steps, and stress some precautions that are required when dealing with high-density fluids.

A. General RHNC method

The principle of the RHNC approximation is to derive from Eq. (1) an expression of the excess free energy, with respect to the HS fluid, by neglecting the variation of the bridge function during the charging process of the perturbation potential. The RHNC free energy is then a functional of the PDF$g(r)$ for the actual interaction, and of the PDF$g_0(r)$ of the HS reference system with adjustable diameter σ. To compute $g(r)$, one uses the OZE,

$$\gamma(r)=\rho\int d\mathbf{r}'\, h(r')c(|\mathbf{r}-\mathbf{r}'|), \tag{7}$$

with $\gamma(r)=h(r)-c(r)$, and $c(r)$ the direct correlation function, the RHNC closure

$$g(r)=\exp[-\beta\phi(r)+\gamma(r)+B_0(r)] \tag{8}$$

and the optimization condition

$$\int d\mathbf{r}[g(r)-g_0(r)]\frac{\partial}{\partial\sigma}B_0(r)=0, \tag{9}$$

where $B_0(r)$ is the reference system [with interaction potential $\phi_0(r)$] bridge function and $\phi(r)$ the total interaction potential. For a given $\phi(r)$, the input data are then the functions $B_0(r)$ and $g_0(r)$.

B. Case of the high-density fluid

$B_0(r)$ and $g_0(r)$ are usually chosen separately from the various parametrizations of existing simulation data. One may, for instance, choose the parametrization of $B_0(r)$ proposed by Malijewsky and Labik (ML) [40], and the Verlet-Weiss one (VW) for $g_0(r)$ [41]. Such a method, however, is acceptable only in the domain of packing fractions, $\eta\leqslant 0.5$, for which these parametrizations were built. In this case indeed, they can be considered as equivalent, since they all reproduce accurately the results of simulations. But this equivalence worsens at higher densities as illustrated in Fig. 1: we compare for a HS fluid with packing fraction $\eta=0.62$ the PDF $g_0^{\mathrm{VW}}(r)$ from the VW parametrization with $g_0^{\mathrm{ML}}(r)$, obtained by solving Eqs. (7) and (8) for the reference HS potential $\phi_0(r)$ with the ML parametrization of $B_0(r)$ [in this case, $g_0^{\mathrm{ML}}(r)$ and $B_0(r)$ are fully consistent]. We see that $g_0^{\mathrm{ML}}(\sigma)>g_0^{\mathrm{VW}}(\sigma)$. This would affect both the RHNC and the FPT results when charging a very-short-range potential. Furthermore, $g_0^{\mathrm{ML}}(r)$ exhibits a secondary peak that is absent in $g_0^{\mathrm{VW}}(r)$ (for a discussion of this peak and its physical consequences, see Ref. [42] and references therein). Our prospect being to study short-range perturbation potentials, only the part of the reference PDF close to the contact is relevant. In this region, we have checked that using Rosenfeld's bridge functional [43] leads to a result very similar to $g_0^{\mathrm{ML}}(r)$. In our calculations, we therefore used the following procedure: at each density, we used as unique input the ML bridge function (which is faster and simpler to evaluate than Rosenfeld's one), and computed $g_0^{\mathrm{ML}}(r)$ as described above.

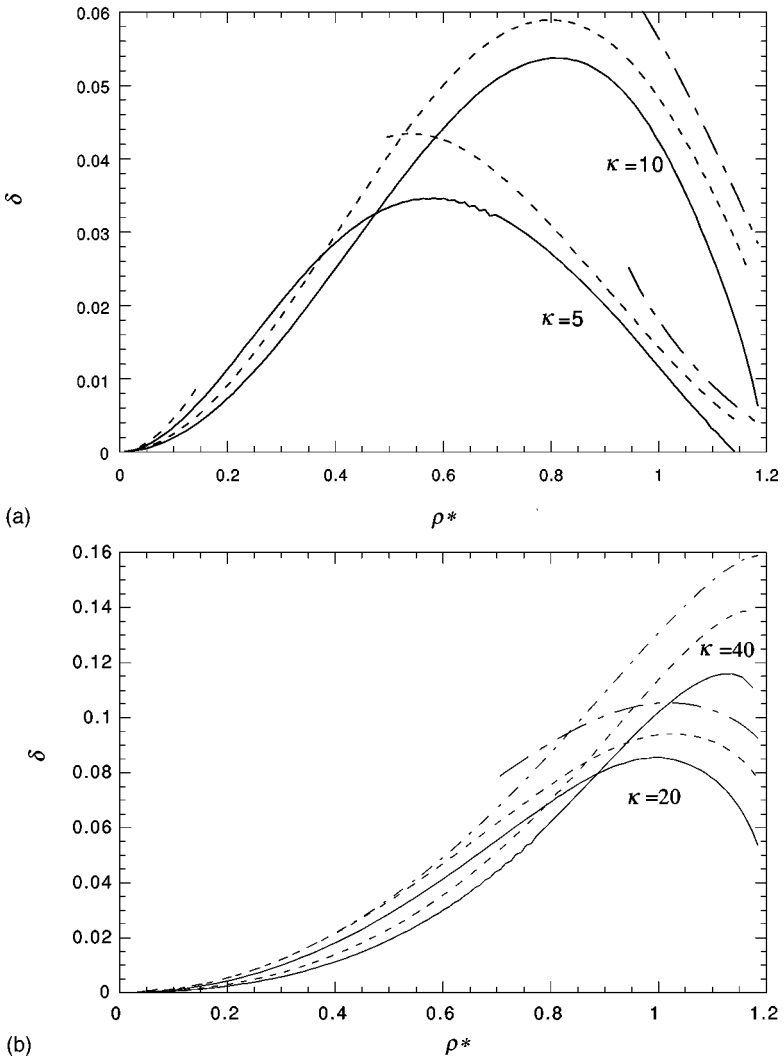

FIG. 2. Influence of the range and reduced strength of the Yukawa perturbation potential on the reduced energy difference $\delta=(\sigma^3/\Omega)\times(\beta\Delta F_1/\epsilon^{*2})$. $\rho^*=\rho\sigma^3$ is the reduced density. (a) $\kappa=5$, 10 with $\epsilon^*=1$ (solid curves), $\epsilon^*=2$ (dashed curves) and $\epsilon^*=4$ (short dash–long dash curves). (b) $\kappa=20$, 40 with $\epsilon^*=1$, 2 and 4 (same symbols). The missing parts in some of the curves correspond to the region of nonconvergence of the optimized RHNC algorithm.

The PDF $g(r)$ corresponding to the total interaction potential was next deduced from Eqs. (7)–(9). This method is computationally less convenient than that using the VW PDF, but is essential at high density to solve the convergence problems of the numerical algorithm one meets when choosing independently $g_0(r)$ and $B_0(r)$ as input (this convergence problem is distinct from that encountered in the intermediate density domain). As a test of the numerical algorithm, we compared our results with those of Caccamo *et al.* [44] for the Yukawa potentials. These authors used a different variant of the RHNC, based on a parametrized bridge function optimized so as to have consistency between the virial and compressibility routes. Our results are in better agreement with simulations than those (already accurate) obtained by these authors. This confirms the opinion [45] that the role of such an imposed consistency is not clear *a priori.*

Finally, the comparison was performed by computing the FPT free energy with the same pair distribution function for the reference system:

$$F^{\rm pert}(\rho)=F_0(\rho)+2\pi N\rho\int_0^\infty dr\, r^2 g_0^{\rm ML}(\tau)V(r). \quad (10)$$

As for the RHNC method, the optimum diameter $\sigma^{\rm opt}$ of the reference system is obtained by minimizing the free energy. For the potential studied in this paper, we found that $\sigma^{\rm opt}$ is systematically that of the physical system.

In the solid, we have computed $F^{\rm pert}(\rho)$ by using the equation of state of Hall [46] for $F_{\rm HS}$ and the parametrization of Kinkaid and Weiss [37] of the averaged HS PDF. We compared the results with the existing MC data [17] for the GED potential.

IV. RESULTS AND DISCUSSION

A. Fluid state

1. Yukawa potential

We first consider the potential

$$\beta\phi(x)=\begin{cases}\infty, & x<1\\ -\varepsilon^*\dfrac{\exp[-\kappa(x-1)]}{x}, & x\geqslant 1\end{cases}$$

(with $x=r/\sigma$) for which the reduced strength ε^* and inverse range κ vary separately. According to Eqs. (2) and (3), the deviation $\beta\Delta F_1$ is of the form $\beta\Delta F_1\sim\varepsilon^{*2}[1+O(\varepsilon^*)]$. We thus computed, for the fluid state, the function δ

TABLE I. Influence of the range and reduced strength of the Yukawa perturbation potential on the PDF contact value $g(\sigma)$.

	$\varepsilon^*=0$	$\varepsilon^*=1$	$\varepsilon^*=2$	$\varepsilon^*=4$
$\kappa=5$	11.37	11.84	12.25	14.34
$\kappa=10$	11.37	15.43	20.87	35.79
$\kappa=20$	11.37	17.37	27.91	60.23

$=(\sigma^3/\Omega)(\beta\Delta F_1/\varepsilon^{*2})$, with Ω the total volume, for different values of κ ($\kappa=5-40$) and ε^* ($\varepsilon^*=1-4$). We restricted ourselves to the region $0<\rho<1.2$ for which it is commonly admitted that a fluid state is defined. For higher density, indeed, the questions relative to the correct description of the disordered state—existence of a ''random close packing'' and exact location—are still in debate (see Ref. [47] and references therein).

Our results are summarized in Fig. 2. We see that, for every couple (κ,ε^*), $\delta(r)$ follows the general behavior discussed in the Sec. II B.

(1) Starting from 0 for $\rho=0$, δ behaves like ρ^2 at low density. In this region, the weaker δ is, the larger κ is.

(2) At higher density, $\delta(r)$ still increases until a maximum value δ_m, after which it decreases. For fixed values of ρ and κ, δ increases with ε^*. However, these variations have a rather small relative magnitude (especially for large κ), for the values of ε^* under consideration: this means that the term in ε^{*2} of the high-temperature expansion [see Eqs. (2) and (3)] is the major contribution to δ. The incorporation of this term could, therefore, bring a significant improvement to the perturbation scheme, at least for the present range of temperature. However, the numerical calculations then become less trivial.

(3) The density ρ_m, corresponding to the maximum deviation δ_m, depends essentially on κ, and it increases with the latter: it is located in the dense fluid region for $\kappa=20-40$ (for $\kappa>40$, ρ_m is outside the region of study) while for $\kappa=5-10$ it is still in the intermediate one (that is, where the fluid-fluid transition usually takes place when it exists). These results are in agreement with our statement of Sec. II B according to which the accuracy of the FPT at high density would be determined, for a fixed value of ε^*, by the respective widths of $f(x)$ and of the main peak of $g_0(x)$.

Another important observation is that δ_m also increases with κ.

Point (3) implies that the FPT is not suitable to describe the liquid phase for large values of $\kappa(\kappa\geqslant 20)$, even at very high density. In Table I, we show indeed that, for a very dense fluid ($\rho^*=1.146$), the RHNC contact value g^0 of the PDF, corresponding to the total potential, strongly differs from that of the HS reference system when passing from $\kappa=5$ to $\kappa=20-40$. It is thus clear that—in the latter cases—the effect of the attractive forces on the structure cannot be neglected as this is done in the FPT.

To evaluate more precisely the consequences induced by the FPT on the *F-F* transition, we next studied the evolution with temperature ($\varepsilon^*=1-4$) of $F^{\text{pert}}(\rho)$ with respect to the ''exact'' free energy $F^{\text{RHNC}}(\rho)$. We considered the two representative cases $\kappa=7$ (Fig. 3) and $\kappa=40$ (Fig. 4). We see that for $\varepsilon^*=1$ (moderate temperature), $F^{\text{pert}}(\rho)$ and $F^{\text{RHNC}}(\rho)$ are almost indistinguishable, even for $\kappa=40$, confirming in a spectacular way our qualitative statement of Sec. II B and previous results from the literature. When increasing ε^*, however, the FTP approximation has quite different consequences according to the value of κ.

$\kappa=7$. The perturbation calculation overestimates the free energy only in the region of intermediate density, the low- and high-density parts being correctly reproduced. As a consequence, the description of the *F-F* transition obtained in the FPT is close to that of the RHNC theory, except in a narrow range of temperature above the actual critical value ($T_c^*\simeq 0.41$): in this region, indeed (see $\varepsilon^*=2.22$) the curve $F^{\text{RHNC}}(\rho)$ is very flat, since the system is close to phase separation. Then the transition exhibited by $F^{\text{pert}}(\rho)$ is only due to the changes of concavity of $\delta(r)$. When using a simple theory, such a discrepancy is not surprising near the

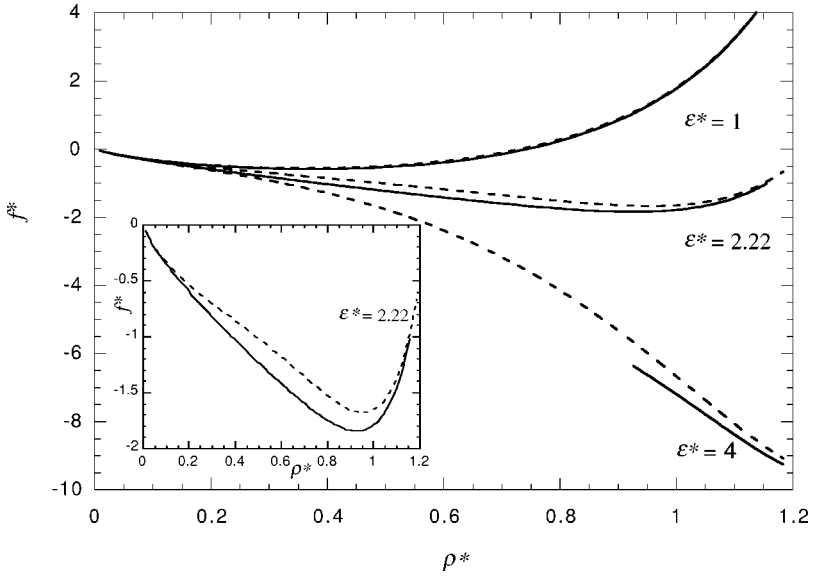

FIG. 3. Evolution with temperature of the reduced free energy $f^*=(\sigma^3/\Omega)\beta F$ for $\kappa=7$. $\rho^*=\rho\sigma^3$ is the reduced density. Solid curve, optimized RHNC. Dashed curve, FPT. Inset shows the *F-F* transition predicted by the FPT for $\epsilon^*=2.22$, just above the actual critical point.

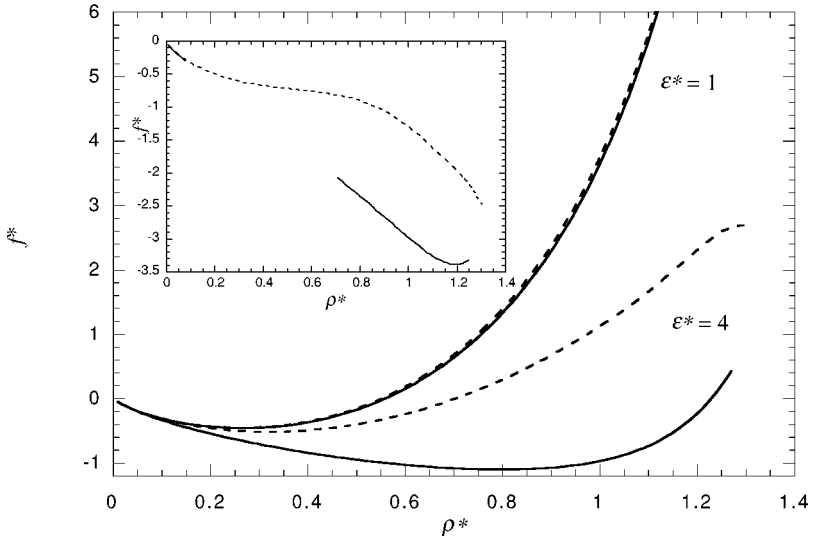

FIG. 4. Evolution with temperature of the reduced free energy $f^*=(\sigma^3/\Omega)\beta F$ for $\kappa=40$. $\rho^*=\rho\sigma^3$ is the reduced density. Solid curve, optimized RHNC. Dashed curve, FPT. The complete discrepancy of the FPT at high density induces an unphysical transition when T is low enough. Inset shows the case $\kappa=20$ for $\epsilon^*=4$ (same symbols).

critical point. As a result, T_c^* is overestimated by about 10% with respect to the MC value (we found $T_c^{*\,\mathrm{pert}}\simeq 0.46$ instead of 0.41 in Ref. [31]). When cooling the system below the critical point, $\delta(r)$ increases. But as ρ_m is well inside the transition region, the densities at coexistence are not significantly modified (see $\varepsilon^*=4$).

Postponing the discussion of the solid phase to the next subsection, the full phase diagram is shown in Fig. 5: we see that the FPT correctly reproduces the *F-S* transition with respect to the RHNC and the MC data, for high as well as for low temperature. For the *F-F* transition, the domain of coexistence is, as expected, a bit overestimated. However, it remains metastable in the FPT as in the RHNC and MC approach (our version of the FPT is therefore slightly better than that used in Ref. [31]).

$\kappa=40$. The situation is completely different for two reasons: the *F-F* transition occurs at much lower temperature (we found $\varepsilon_c^*\simeq 4.6$) and, as emphasized above, the behavior of $\delta(r)$ is much less favorable to the FPT. The consequences are indeed observable for $\varepsilon^*=4$: the difference $F^{\mathrm{pert}}-F^{\mathrm{RHNC}}$ is greater than the variations of F^{RHNC} itself. Moreover, contrary to the case $\kappa=7$, the situation worsens in the dense fluid. The shift of the peak δ_m to higher densities leads to an unphysical transition in the FPT scheme: this would occur at very high density, the upper density branch being out of the accessible domain of study. Such a transition is in fact only the consequence of the variations of $\delta(r)$. An intermediate situation is shown in the inset for $\kappa=20$: just below the critical temperature ($\varepsilon^*=4$), the coexistence densities predicted by the FPT are clearly shifted to higher densities with respect to the RHNC results.

Therefore, the consequences of the perturbation treatment on the *F-F* transition become dramatic for extremely short-ranged interaction: while for $\kappa=7$, the FPT just leads to a slight overestimation of the coexistence domain (we obtained the same result for $\kappa=10$), that corresponding to $\kappa=40$ is qualitatively incorrect and is a pure artifact of the method. Such a failure is very similar to that observed by Velasco, Navascuès, and Mederos [30], who applied the FPT to asymmetric HS binary mixtures in an effective one-component

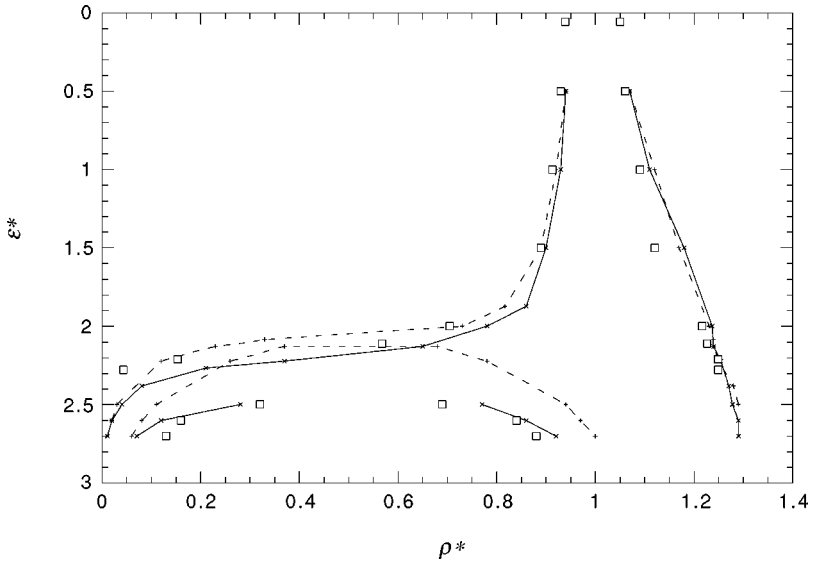

FIG. 5. Phase boundaries of the hard-sphere Yukawa system in the ϵ^*-ρ^* representation for $\kappa=7$. $\rho^*=\rho\sigma^3$ is the reduced density. Solid lines, optimized RHNC (fluid)/FPT (solid). Dashed lines, FPT. Squares, MC [31].

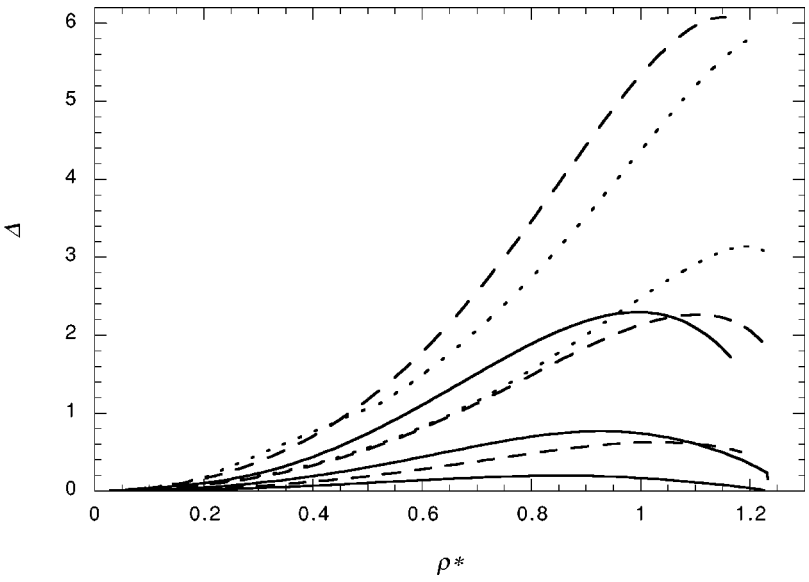

FIG. 6. Influence on the energy difference $\Delta = (\sigma^3/\Omega)\beta\,(F^{\mathrm{pert}} - F^{\mathrm{RHNC}})$ of the size ratio and solvent density for the GED potential. $\rho^* = \rho\sigma^3$ is the reduced density. Solid curves: $q=3$ and $\eta_s = 0.2$ (lower), 0.3 (medium), 0.4 (upper). Dashed curves: $q=5$ and $\eta_s = 0.2$ (lower), 0.3 (medium), 0.4 (upper). Dotted curves: $q=10$ and $\eta_s = 0.2$ (lower), 0.25 (upper).

representation. We will develop this point further in the subsection below.

2. Depletion potential

In the reference quoted above, the FPT was used to study the phase diagram of the mixture for different size ratios ($q=5-20$). This diagram was computed in the plane (η, η_s) for $\eta_s = 0-0.4$, where η is the solute packing fraction, and η_s that of the pure solvent at equilibrium with the mixture. For different versions of the depletion potential [4,8,9], the FPT was compared with the MC results [17], obtained for the same potentials in two cases [8,9] and directly for the mixture in all cases. The most striking result is that while the perturbation satisfactorily reproduces the *F-S* transition, it leads systematically to an artificial *F-F* transition at very high density. This transition is located roughly in the region $\rho > 1$, and is even more shifted for the largest values of q. From the MC data, a *F-F* (metastable) line exists only for the GED potential [8] for a size ratio $q > 10$ (for $q=10$ the transition occurs for $\eta_s = 0.29$). In this case, the coexistence domain is very large, and is located in the more usual region $\rho < 1$. Moreover, concerning the *S-S* isostructural transition line, the FPT reproduces accurately only the high-density branch (see below).

This discrepancy can be explained in a similar way to those obtained with the Yukawa potential for very large κ. To show this, we have plotted $\Delta = \sigma^3/\Omega \times \beta\Delta F_1$ for the GED potential:

$$\beta\phi^G(x) = \begin{cases} \infty, & x < 1 \\ -\dfrac{1+q}{2}\left[3\lambda^2\eta_s + (9\lambda + 12\lambda^2)\,\eta_s^2 + (36\lambda + 30\lambda^2)\,\eta_s^3\right], & 1 \leqslant x \leqslant 1 + \dfrac{1}{q} \\ 0, & x > 1 + \dfrac{1}{q} \end{cases}$$

[with $\lambda = q(x-1)-1$], for $q=3$, 5, 10 and $\eta_s = 0.1-0.4$ (see Fig. 6).

(i) For every couple (q, η_s), $\Delta(\rho)$ has, as expected, the same shape as for the Yukawa potential (for the latter, we plotted $\delta = \Delta/\varepsilon^{*2}$.) This, therefore, explains in the same way why the FPT is more suitable for the *F-S* transition than for the *F-F* one.

(ii) In the present case, the influence of the physical parameters q and η_s on Δ is, however, more complex than that of κ and ε^* for the true one-component systems; indeed, for a fixed q, the increase of η_s not only increases Δ (as does ε^* for the one component fluid), but it also shifts its maximum towards high densities (the same trend is observed when increasing q at fixed η_s). Thus, for every size ratio, there exists a value of η_s above which the FPT will lead to an artificial transition, involving high-density states. This transition is similar to those previously discussed for the large-κ Yukawa systems. But in the present case, it occurs at all diameter ratios. The reason is that, with the depletion potential, the magnitude and the depth of the attractive well do not vary separately with the two parameters η_s and q. This appears in Fig. 7, where $\phi^C(x)$ is plotted for $q=3.5$ and $\eta_s = 0.2$, 0.4: we see that increasing η_s at fixed q increases both the magnitude of ϕ^C at contact and its spatial variations, defined as

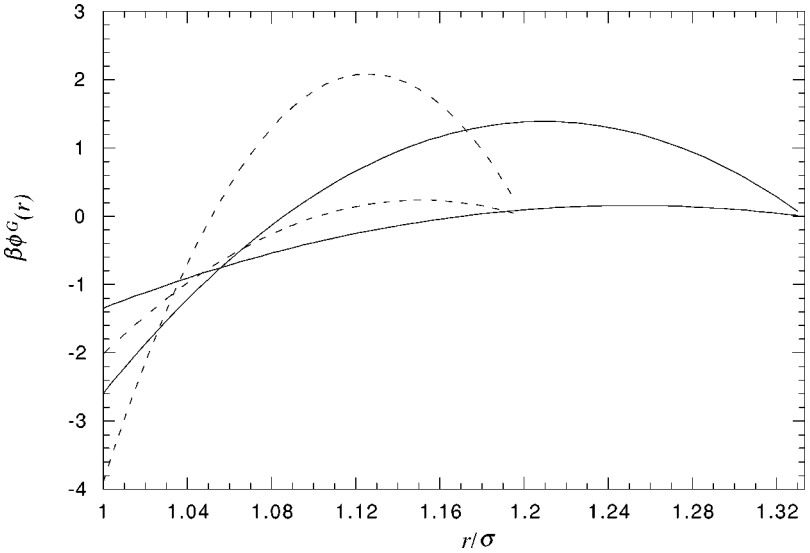

FIG. 7. Dependence of the GED potential on q and η_s. Solid curves: $q=3$ and $\eta_s=0.2$ (lower), 0.4 (upper). Dashed curves: $q=5$ and $\eta_s=0.2$ (lower), 0.4 (upper). For fixed q, the first distance of cancellation of $\phi(x)$ is the lower the greater η_s.

$\Delta x^{-1}=(1/\phi^C)(\partial\phi^C/\partial x)_{x=1}$. For example, for $q=3$, the behavior of $\phi^G(x)$ close to contact (same slope and same magnitude) may be fitted by a Yukawa potential: one gets $(\kappa,\varepsilon^*)\simeq(8,1.34)$ for $\eta_s=0.2$, and $(\kappa,\varepsilon^*)\simeq(14,2.59)$ for $\eta_s=0.4$. As a consequence, the FPT always leads to an unphysical transition, even for moderate size ratio. An example is shown for $q=3$, for which the transition occurs roughly for $\eta_s\simeq0.35$ (see Fig. 8). Finally, we found for greater q the same results as in Ref. [30]: a decrease of the critical η_s, due to the increase of the depletion well, and the shift of the coexistence domain towards the large solute densities, due to the reduction of its depth.

B. Solid state

It is commonly admitted that the perturbation theory is suitable to describe the solid, for which the particles would be closely localized on the lattice sites, and thus the structure rather insensitive to the attraction [30,35]. Indeed, as already mentioned, the FPT reproduces quite well the *F-S* transition even for very singular potentials such as the depletion ones for large asymmetry. However, the situation worsens when considering the *S-S* isostructural transition. This transition exists for hard-core systems with very-short-ranged potential; for instance, it is stable for $q\geqslant20$ for a GED potential [17], and for $\kappa\geqslant25$ for the Yukawa one [33]. For the Yukawa potential, the results obtained in the FPT by Hasegawa [32] were in qualitative agreement with the MC data of Ref. [33], but the critical κ above which the *S-S* transition is stable with respect to melting was somewhat overestimated ($\kappa_c\simeq40$ in the FPT). We found essentially the same result for this potential with our version of the FPT for the fluid and the solid state. But, as there is no (to our knowledge) MC data for the free energy in the literature, we could not push the comparison further.

MC values of the free energy were given in Ref. [17] for the GED potential for $q=5$, 10. The FPT performed in Ref. [30] describes accurately the dense solid branch, near close packing, but not the extended (HS-like) solid one. We argue that this feature, together with the results obtained with the

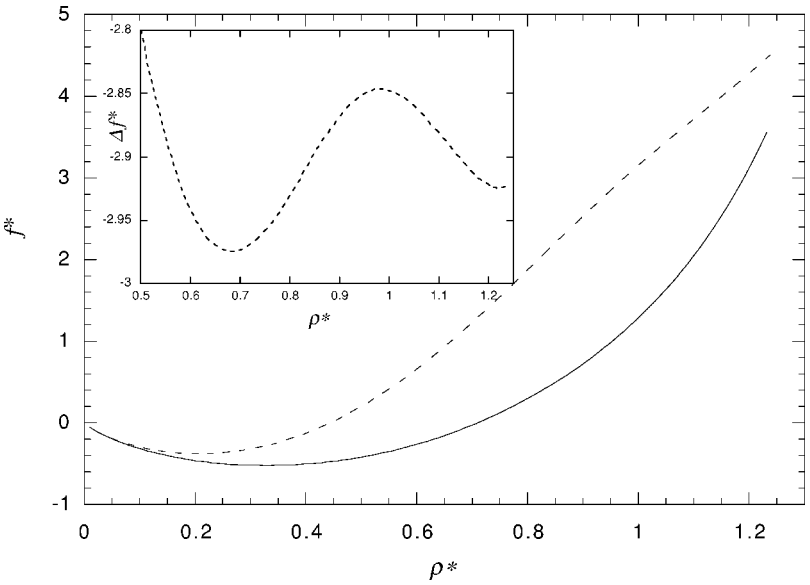

FIG. 8. Influence of the FPT approximation on the *F-F* transition for $q=3$ and $\eta_s=0.38$ [$f^*=(\sigma^3/\Omega)\beta F$ and $\rho^*=\rho\sigma^3$]. At this solvent density, the FPT (dashed curve) leads to an artificial transition that is predicted neither by the optimized RHNC theory (solid curve) nor by the MC simulations [17]. Inset shows the nonlinear contribution to the reduced FPT free energy after subtraction of its linear part.

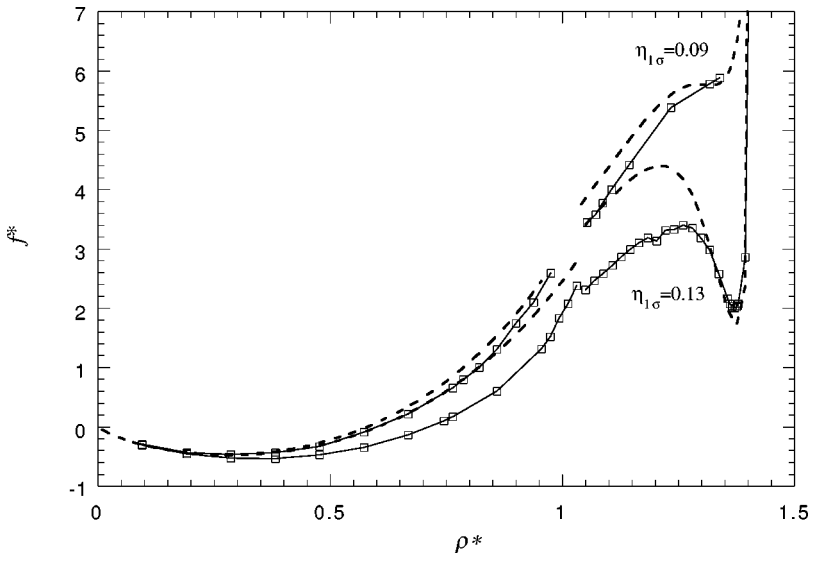

FIG. 9. Influence of the FPT approximation on the reduced solid free energy $f^* = (\sigma^3/\Omega)\beta F$. $\rho^* = \rho\sigma^3$ is the reduced density. The FPT (dashed curve) accurately reproduces the MC data (empty squares, from [17]) only in the dense solid region.

Yukawa potential, is a consequence of the extension of the approximation too far from the close packing limit. This is evidenced in Fig. 9 in which our version of the FPT is compared with the simulations data, for $q=10$ and $\eta_s=0.09$, 0.13. For this size ratio, the *S*-*S* transition is metastable, but its critical point at $\eta_s \simeq 0.06$ is very close to the ''stable'' melting line. While describing rather accurately the minimum of F_{MC} near close packing (due to the very short range of the depletion potential), the deviation ΔF with respect to the simulations increases progressively when decreasing ρ. In both cases, ΔF increases, when passing from the liquid to the solid state. We ignore whether this trend is systematic or not, but it clearly demonstrates that the ordered state is not intrinsically more appropriate for the perturbation treatment. In fact, as emphasized in Sec. II, far from the close packing limit, the averaged two-particle density of the HS solid shows a peak at contact, as in the liquid state. Thus, the accuracy of the FPT is determined in every case by the respective widths of the HS correlation functions and of the interaction potential. When the range of the latter is too short, the FPT cannot be extended to the whole solid region.

However, the high-density solid state is always correctly described since it occurs when the width of the correlation peak is marked enough in the separation range where the potential is significant (see [37,38] for the evolution with density of this peak in the solid). In this case, indeed, the internal energy gain offsets the entropy decrease. This corresponds to the situation where the FPT is appropriate, contrary to the density functional approaches with a liquid state as reference. Moreover, as the *S*-*S* transition occurs for much weaker potentials than the *F*-*F* one, the FTP may be applied close to the critical point in a more suitable way; for instance, we have found the onset of the *S*-*S* transition at $\eta_s = 0.06$ for $q=10$, in agreement with simulations. Our coexistence densities are also correctly located with respect to the MC data ($\rho_c = 1.18$, 1.26 in the FPT, the transition having just occurred). However, as soon as η_s increases, the transition line quickly widens. Then, the extension of the calculation to lower densities makes the FPT inaccurate.

V. CONCLUSION

In this paper, we examined the accuracy of the first-order perturbation theory of classical systems of hard-core particles interacting via short-range attractive potentials. These model potentials may be suitable to describe at the effective one-component level some complex systems such as colloidal suspensions. The advantage of the FPT, in comparison with more accurate methods such as the RHNC for the fluid or the MC simulations, is that it does not require heavy computations and lends itself to simpler interpretations. Furthermore, it is not subject to the nonconvergence problem encountered by most of the integral equation methods when approaching the *F*-*F* coexistence line. Concerning the solid, more sophisticated density functional approaches of the MWDA type involve also heavy computations and are in fact not appropriate for the potentials under consideration in this work.

Our numerical results have been obtained for the Yukawa potential and that of Goetzelman *et al.* They confirm the main trends predicted from our formal analysis: on the one hand, the accuracy of the FPT depends trivially on the temperature, or more generally, the strength of the perturbation potential. In this respect, we have observed for the Yukawa potential that the deviation $F^{\mathrm{pert}} - F^{\mathrm{RHNC}}$ has a major contribution in T^2 in a rather wide range of temperature. This suggests that the accuracy of the perturbation treatment would be improved significantly by incorporating the second-order term. On the other hand, the validity of the FPT depends in a more subtle way on the interplay between the range of the interaction potential and the density of the system: for a fixed potential the difference between the FPT free energy and the ''exact''—RHNC or MC—ones vanishes in the low- and high-density limits while it reaches its maximum at some intermediate value. But while it is commonly considered that the FPT is appropriate to study both the dense fluid and the solid states for potentials with an HS repulsive part, we have shown that this is not true when the range of the attractive tail is very small. Indeed, for very short-range attractions (typically $\kappa \geqslant 20$ for the Yukawa po-

tential) the validity of the FPT is drastically restricted to a very narrow density domain near the close packing limit. The limitation of the FPT for such potentials is a consequence of the strong attractive force they induce near contact: when shifting the density from its close-packing value, these forces quickly compete with the HS repulsion for the determination of the microscopic structure. Then, the HS system is no longer a good reference. Furthermore, we have shown that the accuracy of the FPT is not improved when passing from the fluid state to the solid one with the same density, in contradiction with what could be expected intuitively from considerations based on the density profile of the two states. Indeed, the accuracy of the FPT is in fact determined by the respective widths of the perturbation potential and that of the peak of the PDF—or the averaged one for the solid—near contact. In an extended solid, not at close packing, this peak is not necessarily narrower than that of the fluid with the same density.

To summarize, the FPT is intrinsically suitable to describe the *F*-*S* transition even for extremely short-range potentials. Indeed, this transition involves only physical states for which the FPT is appropriate: moderate strength of the reduced potential for the HS-like transition, and densities very close to the two opposite limits for the sublimation. On the contrary, the prediction for the *F*-*F* transition depends critically on the range of the attraction. For a Yukawa potential, the *F*-*F* transition is qualitatively well described for $\kappa \leqslant 10$, the critical temperature being just slightly overestimated. The situation worsens dramatically for $\kappa \geqslant 20$ where an unphysical transition is found between two high-density fluid states. This failure for such potential ranges is the consequence of the point discussed above. In the case of the depletion potential, we have shown that the FPT leads to a similar artificial *F*-*F* transition whatever the size ratio q is, above some value of solvent packing fraction in the reservoir η_s. In this case indeed, the width of the depletion well may arbitrarily be reduced by increasing η_s at fixed q. Therefore, the pathology of the FPT already observed by Velasco, Navascues, and Mederos for some size ratios is in fact systematically present in the phase diagram. As a consequence, the FPT is not suitable to study the *F*-*F* transition either for pure solvent-colloid systems or for mixture of supramolecular species with moderate size ratio. Furthermore, we have shown that the FPT suffers from the same limitations in the case of the *S*-*S* isostructural transition since this one is present only for very-short-range potentials. The perturbation theory reproduces accurately the solid branch located near close packing but not the extended solid one for which the effect of the attractive forces on the structure cannot be neglected. However, as the *S*-*S* transition occurs for lower strength of the interaction potential, we found that the FPT could eventually be used at least qualitatively to predict the existence of such phase transitions.

[1] L. A. Girifalco, J. Phys. Chem. **96**, 858 (1992).
[2] N. W. Ashcroft, Europhys. Lett. **16**, 355 (1991); Nature (London) **365**, 387 (1993).
[3] J. Q. Broughton and J. V. Lill, Phys. Rev. B **55**, 2808 (1997); C. Caccamo, D. Costa, and A. Fucile, J. Chem. Phys. **106**, 255 (1997).
[4] S. Asakura and F. Oosawa, J. Chem. Phys. **22**, 1255 (1954).
[5] T. Biben and J.-P. Hansen, Phys. Rev. Lett. **66**, 2215 (1991); J. Phys.: Condens. Matter **3**, 65 (1991).
[6] J. L. Lebowitz and S. Rowlinson, Phys. Rev. **41**, 133 (1964).
[7] Y. Mao, M. E. Cates, and H. N. W. Lekkerkerker, Phys. Rev. Lett. **75**, 4548 (1995).
[8] B. Götzelmann, R. Evans, and S. Dietrich, Phys. Rev. E **57**, 6785 (1998).
[9] N. G. Almarza and E. Enciso, Phys. Rev. E **59**, 4426 (1999).
[10] P. Attard, J. Chem. Phys. **91**, 3083 (1989).
[11] T. Biben, P. Bladon, and D. Frenkel, J. Phys.: Condens. Matter **8**, 10799 (1996).
[12] S. Amokrane, J. Chem. Phys. **108**, 7459 (1998).
[13] M. Kinoshita, S. Iba, and M. Harada, J. Chem. Phys. **105**, 2497 (1996).
[14] M. Kinoshita, I. Shin-Ya, K. Kuwamoto, and M. Harada, J. Chem. Phys. **105**, 7177 (1996).
[15] J. Clément-Cottuz, S. Amokrane, and C. Régnaut, Phys. Rev. E **61**, 1692 (2000).
[16] G. Jackson, J. S. Rowlinson, and F. van Swol, J. Phys. Chem. **91**, 4907 (1987).
[17] M. Dijkstra, R. van Roij, and R. Evans, Phys. Rev. E **59**, 5744 (1999).
[18] J-G. Malherbe and S. Amokrane, Mol. Phys. **99**, 355 (2001).
[19] M. Kinoshita, Mol. Phys. **94**, 485 (1998).
[20] J-G. Malherbe and S. Amokrane, Mol. Phys. **97**, 677 (1999).
[21] S. Amokrane and M. Bouaskarne, J. Chem. Phys. **112**, 11 107 (2000).
[22] F. Lado, Phys. Rev. A **8**, 2548 (1973); F. Lado, Phys. Lett. **89A**, 196 (1982); F. Lado, S. M. Foiles, and N. W. Ashcroft, Phys. Rev. A **4**, 2374 (1983).
[23] E. Lomba, Mol. Phys. **68**, 87 (1989).
[24] E. Lomba and N. G. Almarza, J. Chem. Phys. **100**, 8367 (1994).
[25] A. R. Denton and N. W. Ashcroft, Phys. Rev. A **39**, 470 (1989).
[26] A. Kyrlidis and R. A. Brown, Phys. Rev. A **44**, 8141 (1991).
[27] A. R. Denton, N. W. Ashcroft, and W. A. Curtin, Phys. Rev. E **51**, 65 (1995).
[28] C. F. Tejero, M. S. Ripoll, and A. Perez, Phys. Rev. E **52**, 3632 (1995).
[29] D. C. Wang and A. P. Gast, Phys. Rev. E **59**, 3964 (1999); D. C. Wang and A. P. Gast, J. Chem. Phys. **112**, 2826 (2000).
[30] E. Velasco, G. Navascuès, and L. Mederos, Phys. Rev. E **60**, 3158 (1999).
[31] M. H. J. Hagen and D. Frenkel, J. Chem. Phys. **101**, 4093 (1994).
[32] M. Hasegawa, J. Chem. Phys. **108**, 208 (1998).
[33] P. Bolhuis, M. H. J. Hagen, and D. Frenkel, Phys. Rev. E **50**, 4880 (1994).
[34] J. P. Hansen and I. R. Mac Donald, *Theory of Simple Liquids*, 2nd ed. (Academic, New York, 1986); P. A. Egelstaff, *An In-*

troduction to the Liquid State, 2nd ed. (Oxford, New York, 1992); J. A. Barker and D. Henderson, Rev. Mod. Phys. **48**, 587 (1976).
[35] G. Stell and O. Penrose, Phys. Rev. Lett. **51**, 1397 (1983); **52**, 85(E) (1984).
[36] A. R. Denton and H. Löwen, J. Phys.: Condens. Matter **9**, 8907 (1997).
[37] Y. Choi, T. Ree, and F. H. Ree, J. Chem. Phys. **95**, 7548 (1991).
[38] J. M. Kincaid and J. J. Weis, Mol. Phys. **34**, 931 (1977).
[39] K. K. Mon, J. Chem. Phys. **112**, 3245 (2000).
[40] A. Malijevsky and S. Labik, Mol. Phys. **60**, 663 (1987).
[41] L. Verlet and J-J. Weiss, Phys. Rev. A **5**, 939 (1992).
[42] A. Malijevsky, S. Labik, and W. R. Smith, Mol. Phys. **72**, 193 (1991).
[43] Y. Rosenfeld, J. Chem. Phys. **98**, 8126 (1993).
[44] C. Caccamo, G. Pellicane, D. Costa, D. Pini, and G. Stell, Phys. Rev. E **60**, 5533 (1999).
[45] Y. Rosenfeld, J. Phys. Chem. **99**, 2862 (1995).
[46] K. R. Hall, J. Chem. Phys. **57**, 2252 (1972).
[47] S. Torquato, T. M. Truskett, and P. G. Debenedetti, Phys. Rev. Lett. **84**, 2064 (2000).